https://doi.org/10.2352/ISSN.2470-1173.2019.3.SDA-646

StarCAM - A 16K stereo panoramic video camera with a novel parallel interleaved arrangement of sensors

D. E. Meyer [1], ***H. Wang*** [2], ***D. Sandin*** [2], ***C. McFarland*** [1], ***E. Lo*** [1], ***G. Dawe*** [1,2], ***J. Dai*** [1], ***T. Nguyen*** [1], ***H. Baker*** [3], ***M. D. Brown*** [2], ***T. DeFanti*** [1,2], ***F. Kuester*** [1]

[1]University of California San Diego; La Jolla, CA

[2]Electronic Visualization Laboratory, University of Illinois at Chicago; Chicago, IL

[3]EPIImaging LLC; Los Altos, CA

Abstract

The most common sensor arrangement of 360 panoramic video cameras is a radial design where a number of sensors are outward looking as in spokes on a wheel. The cameras are typically spaced at approximately human interocular distance with high overlap. We present a novel method of leveraging small form-factor camera units arranged in stereo pairs and interleaved to achieve a fully panoramic view with fully parallel sensor pairs. This arrangement requires less keystone correction to get depth information and the discontinuity between images that have to be stitched together is smaller than in the radial design. The primary benefit for this arrangement is the small form factor of the system with the large number of sensors enabling a high resolving power. We highlight mechanical considerations, system performance and software capabilities of these manufactured and tested imaging units. One is based on the Raspberry Pi cameras and a second based on a 16 camera system leveraging 8 pairs of 13 megapixel AR1335 cell phone sensors. In addition several different variations on the conceptual design were simulated with synthetic projections to compare stitching difficulty of the rendered scenes.

Introduction

Panoramic images and videos give users the benefit of an increased field of view at equal spatial resolution than single view cameras [5]. The field of Panoramic Computer Vision has had an abundance of monocular panoramic research demonstrating the feasibility of merging neighbouring images and image sequences into single, stitched panoramas [6]. Application domains like Virtual Reality, Cinematography and Autonomous Robotics have fostered the need to develop stereoscopic systems, capable of capturing, stitching and rendering stereoscopic panoramic views. Industrial camera systems such as the ones by Facebook [13] and Google Jump [2] have proposed the solution in the form of a high-overlap spoked designs, where individual camera focal points are roughly at inter-ocular distance. All re-projection occurs in software, where the left and right viewpoints are synthesized [14]. This inherently introduces induces two problems: a loss of resolution due to stereo keystoning of non-parallel cameras; and a large physical camera layout to maintain the disparity for the stereo re-projection [14]. We propose an alternative design, based on the patented parallel interleaved camera design [17][3], where pairs of camera are radially iterated to address these limitations of spoked camera designs. Interleaving the cameras additionally provides the benefit that the panels that need to be stitched together is one half the inner ocular distance while in the spoked design, the panels that need to be stitched together have a disparity equal to the inner ocular distance.

This paper addresses the qualitative comparison between radial and parallel interleaved camera layouts for stereo-panoramic cameras, as illustrated in Figure 1. We evaluate the stitching comparison between both design approaches for synthetic data, and evaluate results for two iterations of a physical camera layout with the parallel interleave design. We illustrate the system and results of the novel StarCAM parallel interleave design that achieves 20/20 acuity when driven at the full resolution.

Motivation

A predominant demand for high-resolution stereoscopic, panoramic video is Virtual Reality. Many head-mounted displays lack the native resolving power of human vision, and with it, user-content lacks these resolutions too [4]. Immersive CAVE systems [7] have pioneered visualization into high-resolution scenes and have gotten to the point of exceeding human resolving power, driving the need for high resolution stereo-panoramic data. This work has been largely driven in parallel to the CAVE development such that high resolution stereo-panoramic video data can be used within them.

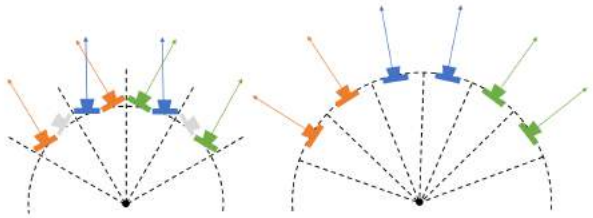

Figure 1: Design comparison between parallel interleave and radial/spoke camera layout

Stereo Panoramic Video

Panoramic images have horizontally elongated fields of view which are created through either mosaicing of smaller field-of-view (FOV) images [18], sweeping of line-sensors [10] or high-optical distortion lens systems which allow a full or partial viewing circle to be captured [12]. The major difference in system manifesting themselves in system size, frame capture-rate and angular resolving power. Sweeping line-sensors lack the ability to achieve video frame-rates of 30 Hz and single sensor, high FOV systems do not achieve the desired resolution, as such we will ad-

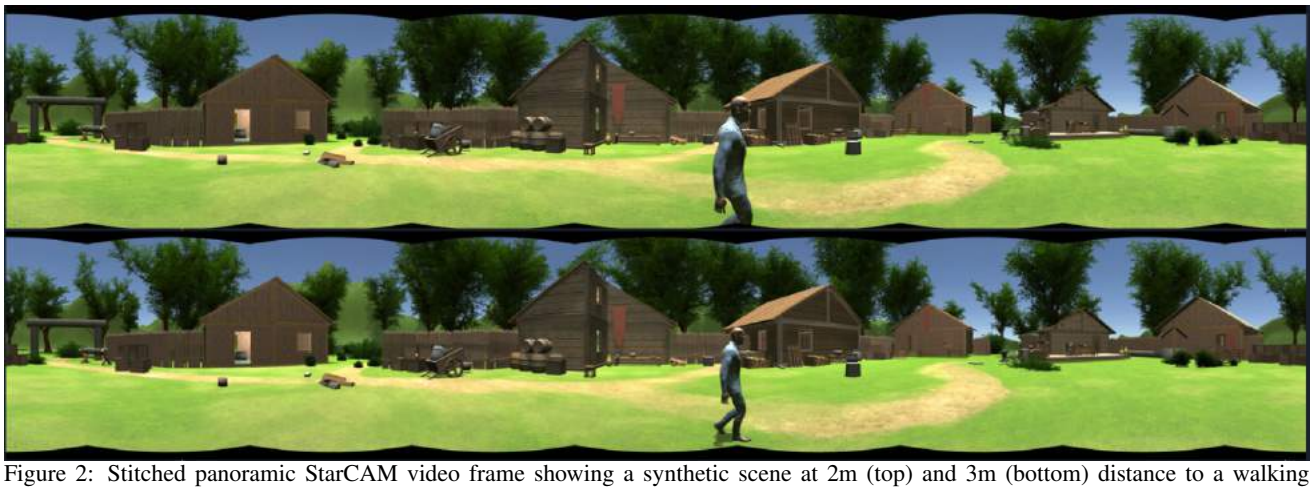

Figure 2: Stitched panoramic StarCAM video frame showing a synthetic scene at 2m (top) and 3m (bottom) distance to a walking character

dress the mosaicing approach of multiple individual images captured about a central pivot point to achieve panoramic vision.

To achieve stereoscopic scene captures, the viewpoint must be captured with focal points of cameras that have a certain disparity to achieve parallax. Few attempts of monoscopic reprojections into stereocopic scenes have shown feasibility [11], but certain scene occlusions do require original capture to be correctly synthesized [9]. Stereoscopic panorama images have been successfully generated using a stereo camera pivoted around the center of the baseline as shown in [16], which works well for stills but cannot scale to video frame-rates. To achieve this desired video rate scene capture, a camera array must be used to capture multiple viewpoints simultaneously in a synchronized fashion [3]. The predominant stereo panoramic cameras use a radial spoke design with high-overlap to achieve horizontal disparity and hence stereoscopic scene capture [14]. Figure 3 illustrates the stereo ray casting for a set of spoked cameras, applicable also to the interleaved design, based on the original work of Peleg et al. [14]. This was further expanded by Richardt et al. [15] for high resolution panoramas where continuities are preserved between individual panoramas (reduced seam-lines) and stereo pairs (pleasant stereo for viewer).

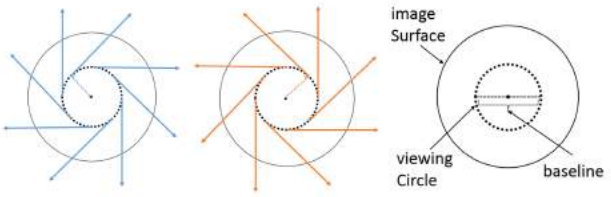

Figure 3: Stereo panoramic viewpoint projection

The stereoscopic video scenes from cameras with a disparity introduce a set of inherent stitching difficulties due to the parallax. For monoscopic panoramas, the viewpoint is optimally rotated about the focal point, whereas with stereo pairs, the rotation point is about the baseline center. For stereo-panoramic video multiple cameras must be used so it is not possible to rotate the cameras about their focal points or baseline center, forcing a rotation about a point behind the center of the baseline (Figure 1). This induces a non-optimality for individual left and right panorama stitching because of the parallax. As we will discuss in [section stitching software], the combined disparity and layout of video stereoscopic panoramic cameras creates the following stitching difficulties:

- Consistency of features in the individual monoscopic panoramas (2D stitching errors).
- Coherence between stereo panorama pairs (correct stereo vision).
- Consistency of stitches in the time-domain for the panoramas (video correctness).

Synthetic Design Evaluation

We propose two designs of a panoramic video array which leverages small form factor cell-phone cameras: one as a spoked array and the other as a parallel interleaved one. For purposes of simplicity we will label these SpokeCAM and StarCAM respectively. Both have equivalent stereo baselines, however the layout creates significantly different overall array sizes. For comparison, we propose both of these arrays in synthetic form- a CAD driven layout which was re-created in Unity to generate sample data in a virtual, moving world. The system parameters mimic the AR1330 sensor cellphone modules in the Econsystems CU130 [1] cameras such as to accurately replicate the StarCAM physical camera in section [section camera]. We adopt one minor modification in the design which is to increase the vertical FOV of the synthetic camera such as the aspect ratio is square. This measure was to improve visual stitching evaluation in the CAVE systems, and does not in anyway affect the quantitative and qualitative comparisons we evaluate.

For each test sequence, we rendered 300 frames to simulate

Array	Camera Number	Stereo Baseline (mm)	Array Diameter (mm)	Field-of-View (deg)	Camera Spec
SpokeCAM	16	75	385	360 x 60	AR1330, 1920 x 1080
StarCAM	16	75	160	360 x 60	AR1330, 1920 x 1080

Table 1: SpokeCAM and StarCAM array specifications

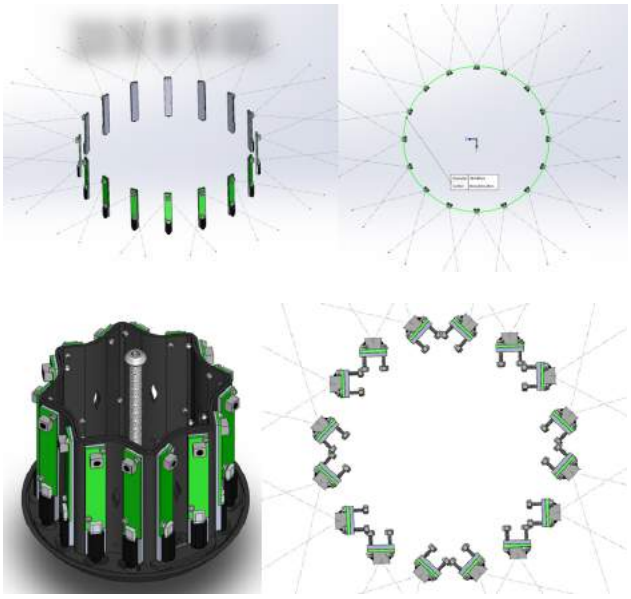

Figure 4: SpokeCAM: side-view (a), top-view (b). StarCAM: side-view (c), top-view (d).

a 10 second, 30FPS capture. We use two scenes for each camera which differ only in the distance at which a walking man walks around the camera- 2 and 3 meters respectively. The scenes consist of an outdoor set with static buildings, bushes and diverse objects, all of which are at distances greater than the walking man. The evaluation of both camera arrays are based on these synthetic viewpoints, which are stitched in panoramic videos with each frame being a panorama as in Figure 2.

Stitching Algorithm

Panoramic image and video stitching is commonly approached in two methods: 1) feature based alignment of frames with best-fit warping and blending, and 2) scene estimation and full re-projection with blending. We selected the first of the two as a means to evaluate the performance of these two systems.

A set of features are extracted from each frame and matched to the neighbouring images and to the frames before and after the concerned frame using the common feature based stereo algorithm [20]. This guarantees both spatial and temporal consistency of the features. We describe all features consistent across multiple frames as Commonly Identified Features (CIF), which will serve as the sparse backbone to the analysis. Using a depth-constraint, we are then able to track these features with the Kanade-Lucas-Tomasi feature tracker to ensure that areas closer (showing more motion between frames) require more feature updates than the static background. Following the feature tracking, we use a depth aware image alignment method that uses the RANSAC-based homography estimation to align image areas and blend them together. This stitching method is based on works [21][20].

CIF Error Analysis

To evaluate the stitching quality of frames from both arrays, we use a monoscopic and binocular stitching quality error metric. This serves to evaluate the feature consistency across overlapping frames and stereo pairs. A CIF is observed in four neighbouring images (two interleaved camera pairs). We will use P_1, P_3 for the left and right cameras of the first pair and similarly, P_2, P_4 for the second pair. We define a feature correspondence of these features into the stitched panorama such as to produce a projected feature set $\{P'_1, P'_2, P'_3, P'_4\}$. We define the error of corresponding features in just the left frames and panoramas, followed by those in the right frames as described in Equations 1 and 2.

$$Error_{left} = \frac{1}{N}\Sigma_{i=1}^{N}(\sqrt{((P_1^i x - P_2^i x)^2 + (P_1^i y - P_2^i y)^2}) \quad (1)$$

$$Error_{Right} = \frac{1}{N}\Sigma_{i=1}^{N}(\sqrt{((P_3^i x - P_4^i x)^2 + (P_3^i y - P_4^i y)^2}) \quad (2)$$

A horizontal pixel disparity from the CIF can be defined from both the original left and right images d_1, d_2, which corresponds to a pixel disparity across the left and right stitched panoramas. We expect the horizontal pixel disparities to be identical in the original and stitched panoramas, however, disagreements between these values serve as an error metric to evaluate the stitchability of these features as is defined in Equations 3 and 4. This can similarly be applied to the vertical disparity (Equations 5 and 6), which we expect to be zero for both camera arrays. We perform a normalized error measurement across all overlapping camera pairs, and across all frames over time to evaluate this disparity agreement.

$$Error_{hor,left-side} = \frac{1}{N}\Sigma_{i=1}^{N} abs((P_1^i x - P_3^i x) + (d_1^i x - d_3^i x)) \quad (3)$$

$$Error_{hor,right-side} = \frac{1}{N}\Sigma_{i=1}^{N} abs((P_2^i x - P_4^i x) + (d_2^i x - d_4^i x)) \quad (4)$$

$$Error_{ver,right} = \frac{1}{N}\Sigma_{i=1}^{N}\sqrt{(P_1^i y - (P_3^i y)^2} \quad (5)$$

$$Error_{ver,left} = \frac{1}{N}\Sigma_{i=1}^{N}\sqrt{(P_2^i y - (P_4^i y)^2} \quad (6)$$

The monocular CIF error for both the StarCAM and SpokeCAM with the walking man at 2m and 3m is shown in Figure 5. For the binocular pixel disparity error, the results are shown in Figure 6. Due to the low mean error values, the high standard deviation, and similarity in between the two array erros, we decided to proceed with a T-Test to conclude the statistical significance of these Table 2.

T-test	Left Monocular Error- 2m	Right Monocular Error- 2m	Left Monocular Error- 3m	Right Monocular Error- 3m
SE	2.0986	2.0432	0.026	0.0266
DF	6682	6682	6842	6842
T-score	44.9349	12.7852	48.238	13.2113
P-value	0<0.05	2.6844e-37<0.05	0<0.05	1.1429e-39<0.05
Conclusion	StarCam mean error is smaller	StarCam mean error is smaller	StarCam mean error is smaller	StarCam mean error is smaller

Table 2: T-Test results for monoscopic CIF error comparison of SpokeCAM and StarCAM

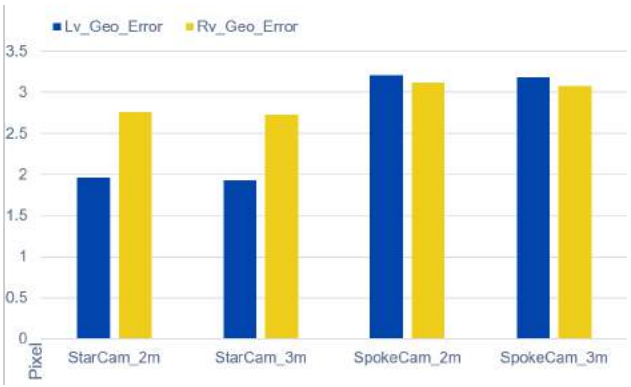

Figure 5: Monocular CIF error

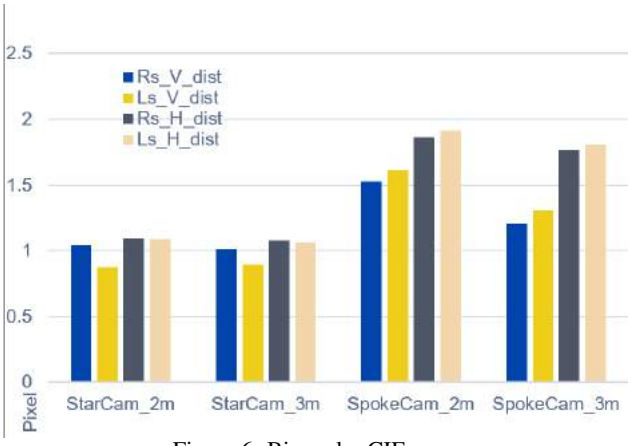

Figure 6: Binocular CIF error

Visual Stitching Evaluation

While the error measurements outlined in the previous section provide a quantitative evaluation of the stitching performance comparison, they do not capture visible stitching seams, which in the case of panoramic image stitching provide the greatest noticeable issue to the viewer [19]. We also completed a visual inspection of the 2M and 3M cases (100 frames each) and focused on the regions where the walking man crosses two sets of scenes: region A and B respectively. For all these stitched frames, we visually inspected to identify any stitching errors and classified each frame as good or bad. The results are shown in Table 3. Combining both region statistics, StarCAM achieves a good to bad frame ratio of 94% while SpokeCAM only achieves 73% for the 2M case and 100% and 75% respectively for the 3M case. We can conclude that the StarCAM design has less visibly apparent stitching issues compared to the SpokeCAM in this test.

Region		StarCAM		SpokeCAM	
		Good	Bad	Good	Bad
A (47 frames)	2m	47	0	35	12
B (37 frames)		32	5	26	11
A (18 frames)	3m	18	0	3	15
B (63 frames)		63	0	58	5

Table 3: Overlap seam visual inspection for 2M StarCAM and SpokeCAM tests

Synthetic sArray Performance Discussion

We have proposed both a quantitative and qualitative evaluation for the stitching quality of synthetic image sets for the two camera arrays. The CIF based comparison showed minimal average errors around 1-2 pixels, with the StarCAM demonstrating a lower error. Due to the high standard deviation and similarity in the SpokeCAM we used a T-Test (Table 2) to validate the result comparison. With a negligibly small P-Value in both left and right stitches, we accept the hypothesis that the StarCAM demonstrates a lower error than the SpokeCAM with a statistical significance greater than the 95th percentile. It is however to be noted that due to the small error values, it is inconclusive whether these results reflect visible stitching anomalies and appropriately justify the advantageous layout of the StarCAM. The visual evaluation of the stitches confirm better performance with the StarCAM than with the SpokeCAM, confirming the findings from the CIF errors. These assumptions hold for the stitching method described in Section , but may difer in other methods.

Parallel Interleaved Camera Development

The synthetic array design motivated a real-world implementation of the parallel interleaved camera design. The major requirement being the small form factor of the cameras which would allow tight packaging into the parallel interleaved design. This section addresses the design choices and system integration of two such camera systems.

Figure 7: Camlot camera prototype with RPI boars

Figure 8: Camlot stitching sample from 3 stereo pairs

Camlot Prototype

A preliminary design leveraged 8 Raspberry Pi Cameras paired with a raspberry Pi each, Figure 7. This was a partial panoramic ring which used 4 parallel, stereo pairs. The cameras were able to capture 1080p frames at 30 fps, yet lacked the

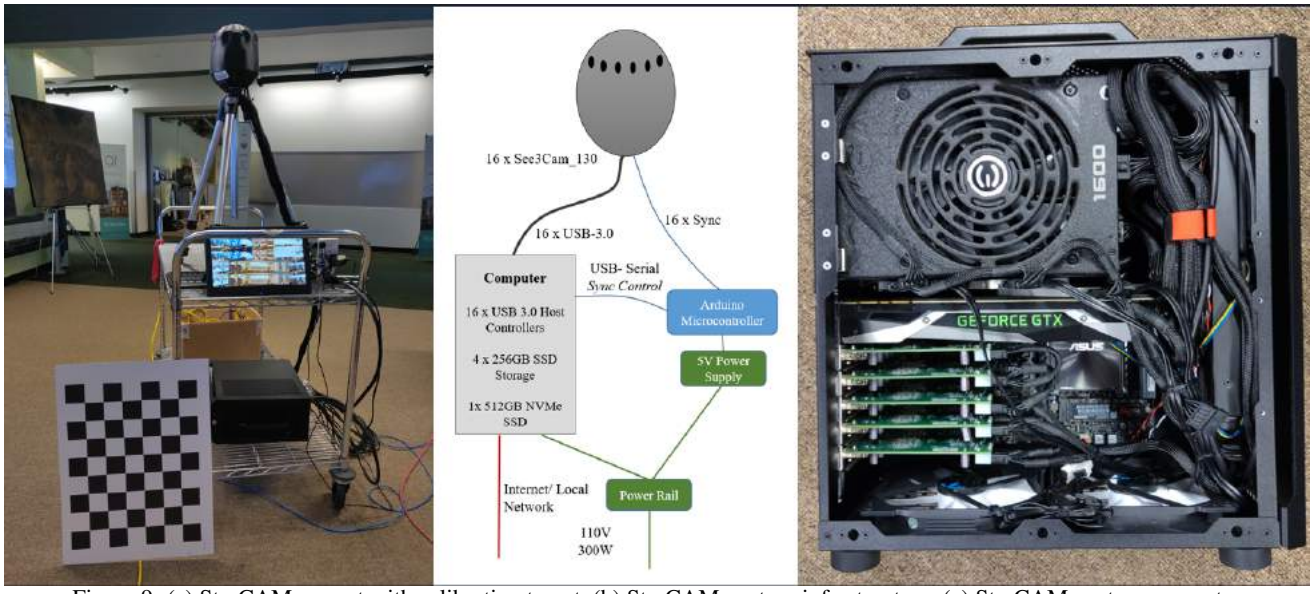

Figure 9: (a) StarCAM on cart with calibration target, (b) StarCAM capture infrastructure, (c) StarCAM capture computer

ability for the separate cameras to be synchronized. The rolling shutter sensors would exhibit a substantial time-delay between the cameras when the frames were triggered which would make the system unfeasible to use in moving, dynamic scenes. We successfully produced static stereo panoramas, such as that in Figure 8.

StarCAM Camera

Availability of cell phone cameras fostered the integration of these in devices other than cellphones. The Econsystems 130 [1] camera adapts the MIPI-CSI sensor to USB3.0, a widely usesd interface which allows for camera control over DirectShow or Video4Linux APIs. Furthermore, these cameras feature a External Synchronization ability, where the pixel row readout is synchronized between the camera, allowing for the best possible rolling shutter synchronization. The sensor size is 13 Megapixels (limited at 12FPS), but the camera allows for faster frame-rates at 4K resolution (30FPS) and 1080p resolution (60FPS). Due to capture stability issues at higher datarates, we drive the cameras at 1080p, 30 FPS.

The StarCAM array (Figure 9) uses 8 parallel camera pairs (16 cameras total) to complete a full horizontal view circle. The horizontal baseline of the pairs is chosen at 75mm to optimize overall layout, and to resemble human Inter-Ocular Distance (IOD). Due to a narrow vertical FOV of the camera modules, we are limited to 30 degree vertical FOV in the panoramas. Future designs may leverage multiple stereo rings to increase this FOV.

Due to the data-rate requirements of these USB 3.0 cameras, we used a dedicated USB 3.0 Host Controller per camera, for the option of maximizing the data-rate that the camera can provide. We were able to pair multiple cameras per host-controller for lower-resolution and frame-rate captures. Figure 9 shows the assembled StarCAM array with it's capture computer. The custom recording software which was developed interfaced with all cameras over the DirectShow API, and synchronized the capture settings (exposure, focus, gain, white balance and external trigger) across all cameras. All frames are received into a frame buffer and flushed to disk, while also being downsampled for a live capture preview. No real-time stitching is being performed on the computer in its current iteration.

The StarCAM array requires a calibration to correct for optical and physical system misalignments. We use a 2x3 foot checkerboard that is radially rotated about the camera while frames are being saved. Emphasis is provided on acquiring many frames while the checkerboard is in the overlapping region. A Matlab camera solver is used to derive intrinsic and extrinsic parameters for the array cameras. All scene capture frames are rectified from these parameters before the stitching method is applied. All stitching of the real-world data follows the same stitching pipeline that is described in Section . For evaluation purposes we completed three types of acquisition tests:

1. Stationary camera array with people walking around it.
2. Rotating camera array with people walking around it.
3. Moving camera on top of a car.

Physical StarCAM Stitching Results

The stitches completed from the physical StarCAM data resulted in stereo video clips of varying length. Due to the high resolution of the output videos, we used CAVE systems to visually evaluate these as alternative methods did not allow for one-to-one resolution viewing. A sample frame from the stitched StarCAM video data which was evaluated is shown in Figure 10.

Two of the authors along with undergraduate research assistants evaluated several test sequences of StarCAM panoramas in the CAVE2 [8] at the Electronic Visualization Laboratory, University at Illinois-Chicago. The first impression was the pleasant sharpness of the image in comparison to lower resolution 4K and 6K panoramas from commercial panoramic cameras. These lower resolution cameras look very soft in the CAVE2 which has 20/20 acuity. In addition the motion from StarCAM data was smooth, the stereo viewing was very comfortable and it took several repeated viewings before people began to see some of the stitching issues. The group also viewed the eye charts that were embedded in the scene and reported 20/40 acuity. Across the video sets,

Figure 10: Outdoor monoscopic panorama from left 8 cameras of StarCAM

multiple viewers at the University of California San Diego arrived at a general consensus that the stereo viewing was pleasant, with the resolution being uniform around the FOV of the output. All scenes were subject to stitching artifacts when moving objects crossed camera pair seams, with the biggest errors manifesting themselves with close objects. The visual acuity of the system was confirmed with an eye target at 20/40 during the 1080p per camera output, and at 20/20 for a still frame with 4K resolution per camera. Synchronization of the cameras was confirmed with a flash triggered at the beginning and end of the sequences. Frame counts showed that frame drops are sparse but existent over multi-minute captures. Greater stability was observed when the cameras within StarCAM were driven at 1080p per camera at 30 FPS compared to when they were driven at 4K resolution.

Conclusion and Future Works

This paper has introduced the concept of a parallel interleaved arrangement of sensors to create a compact stereo-panoramic video camera. We have compared a synthetically generated dataset from both the StarCAM design, as well as its radial equivalent, SpokeCAM. Through the use of CIF error measurements, we were able to conclude that the StarCAM allows for smaller errors in both 2m and 3m walking man cases. Furthermore, visual inspections confirmed the advantageous stitching with the StarCAM layout for the given stitching approach proposed. While our analysis has supported the parallel interleaved design over the spoked radial design, we recognize that this is largely subject to the stitching algorithm used and that many commercial radial arrays have produced excellent results. A physical implementation of the StarCAM design was created to evaluate the design in real world scene captures. Stitching results, while prawn to anomalies, demonstrated a pleasure viewing experience when evaluated by domain field experts.

Future improvements to the system include improving the stability at the full camera video resolution- 4K, 30FPS for recording which is at this point still unstable. Additionally, development of the stitching method that leverages better scene estimation is required to evaluate the stitching quality. In scene estimation, we require 3D depth perception as a common metric to evaluate performance which can be applied to this system in future works. A large requirement is hardware accelerating such estimation, which would likely be done on FPGAs or GPUs. We hope to further the development of the StarCAM system to accommodate larger vertical FOVs and stereo baselines, which requires an increase of camera numbers and array size.

Acknowledgments

This publication is based on work supported by the National Science Foundation (NSF) award #CNS-1456638 for SENSEI, the US Army Corps of Engineers under research Cooperative Agreement W912HZ-17-2-0024, NIST Award #70NANB17H211, as well as NSF award #CNS-1338192, MRI: Development of Advanced Visualization Instrumentation for the Collaborative Exploration of Big Data. Additional support was provided by the Kinsella Expedition Fund, the Qualcomm Institute at UC San Diego and the World Cultural Heritage Society. We also would like to express our appreciation for the significant contributions of Ahmad Atra, Serena Schultz, Hayley Christianson and Bartosz Kupiec as part of the NSF Research Experiences for Undergraduates (REU) program. We thank all collaborators in Calit2, UC San Diego, as well as all other contributors to ideas, suggestions and comments of this work. Opinions, findings, and conclusions from this study are those of the authors and do not necessarily reflect the opinions of the research sponsors.

References

[1] Anon. Econsystems see3cam130 camera board, *https://www.e-consystems.com/*.

[2] Anon. Google jump vr camera, *https://vr.google.com/jump/*.

[3] Henry Harlyn Baker and Papadas Constantin. Panoramic stereoscopic camera, May 3 2012. US Patent App. 12/914,771.

[4] Doug A Bowman and Ryan P McMahan. Virtual reality: how much immersion is enough? *Computer*, 40(7), 2007.

[5] Matthew Brown and David G Lowe. Automatic panoramic image stitching using invariant features. *International journal of computer vision*, 74(1):59–73, 2007.

[6] Li-huan CAI, Ying-hao LIAO, and Dong-hui GUO. Study on image stitching methods and its key technologies [j]. *Computer Technology and Development*, 3:002, 2008.

[7] Carolina Cruz-Neira, Daniel J Sandin, and Thomas A DeFanti. Surround-screen projection-based virtual reality: the design and implementation of the cave. In *Proceedings of the 20th annual conference on Computer graphics and interactive techniques*, pages 135–142. ACM, 1993.

[8] Alessandro Febretti, Arthur Nishimoto, Terrance Thigpen, Jonas Talandis, Lance Long, JD Pirtle, Tom Peterka, Alan Verlo, Maxine Brown, Dana Plepys, et al. Cave2: a hybrid reality environment for immersive simulation and information analysis. In *The Engineering Reality of Virtual Reality 2013*, volume 8649, page 864903. International Society for Optics and Photonics, 2013.

[9] Duke Gledhill, Gui Yun Tian, Dave Taylor, and David Clarke. Panoramic imaginga review. *Computers & Graphics*, 27(3):435–445, 2003.

[10] Fay Huang, Reinhard Klette, and Karsten Scheibe. *Panoramic imaging: sensor-line cameras and laser range-finders*, volume 11. John Wiley & Sons, 2008.

[11] Jingwei Huang, Zhili Chen, Duygu Ceylan, and Hailin Jin. 6-dof vr videos with a single 360-camera. In *Virtual Reality (VR), 2017 IEEE*, pages 37–44. IEEE, 2017.

[12] Gurunandan Krishnan and Shree K Nayar. Cata-fisheye camera for panoramic imaging. In *Applications of Computer Vision, 2008. WACV 2008. IEEE Workshop on*, pages 1–8. IEEE, 2008.

[13] David Lindell and Jayant Thatte. Virtual reality motion parallax with the facebook surround-360.

[14] Shmuel Peleg, Moshe Ben-Ezra, and Yael Pritch. Omnistereo: Panoramic stereo imaging. *IEEE Transactions on Pattern Analysis and Machine Intelligence*, 23(3):279–290, 2001.

[15] Christian Richardt, Yael Pritch, Henning Zimmer, and Alexander Sorkine-Hornung. Megastereo: Constructing high-resolution stereo panoramas. In *Proceedings of the IEEE Conference on Computer Vision and Pattern Recognition*, pages 1256–1263, 2013.

[16] Neil G Smith, Steve Cutchin, Robert Kooima, Richard A Ainsworth, Daniel J Sandin, Jurgen Schulze, Andrew Prudhomme, Falko Kuester, Thomas E Levy, and Thomas A DeFanti. Cultural heritage omni-stereo panoramas for immersive cultural analytics–from the nile to the hijaz. In *Proceedings of the 8th International Symposium on Image and Signal Processing and Analysis, Trieste, Italy*, pages 552–57, 2013.

[17] Leonard P Steuart III. Digital 3d/360 camera system, February 25 2014. US Patent 8,659,640.

[18] Richard Szeliski et al. Image alignment and stitching: A tutorial. *Foundations and Trends® in Computer Graphics and Vision*, 2(1):1–104, 2007.

[19] Michael W Tao, Micah K Johnson, and Sylvain Paris. Error-tolerant image compositing. In *European Conference on Computer Vision*, pages 31–44. Springer, 2010.

[20] Haoyu Wang, Daniel J Sandin, and Dan Schonfeld. A common feature-based disparity control strategy in stereoscopic panorama generation. In *Visual Communications and Image Processing (VCIP), 2017 IEEE*, pages 1–4. IEEE, 2017.

[21] Haoyu Wang, Daniel J Sandin, and Dan Schonfeld. Saliency-based feature selection strategy in stereoscopic panoramic video generation. In *2018 IEEE International Conference on Acoustics, Speech and Signal Processing (ICASSP)*, pages 1837–1841. IEEE, 2018.

Author Biography

Dominique Meyer received his B.S. in Physics at the University of California San Diego in 2017 and is currently pursuing his Ph.D. in the department of Computer Science and Engineering working with Professor Kuester and Christensen. He is part of the Contextual Robotics Institute, and focuses on the development of imaging systems for autonomous ground and aerial vehicles.

Haoyu Wang is a PhD candidate in the Department of Electrical and Computer Engineering at University of Illinois at Chicago. He works as Research Assistant for SENSEI (SENSor Environment Imaging) project in Electronic Visualization Laboratory since 2015. In this project, he mainly focuses on the construction of efficient and automatic stereoscopic panorama stitching system. His current work includes panorama depth correction, stitching quality evaluation and generation of the stereoscopic 360 video.

Daniel Sandin is director Emeritus of the Electronic Visualization Lab (EVL) and a professor Emeritus in the School of Art and Design at the University of Illinois at Chicago (UIC). Currently Sandin is a visiting senior research scientist at EVL. Sandin is particularly interested in the creation of VR artworks that involve the natural world and as built environment, camera image materials, rich human interaction and mathematical systems.

Christopher McFarland is a staff software engineer at UC San Diego. He received his B.S. in Computer Science in 2012 and has since worked on research projects including: spherical video capture and playback, long-term preservation of research data, and large-scale virtual reality display systems.

Eric Lo is a Development Engineer at the Qualcomm Institute at UC San Diego. He received his B.S. in 2015 in the department of Electrical and Computer Engineering and the UC San Diego. His interest is in developing and optimizing autonomous robotic platforms for high resolution, large scale data acquisition, from centimeter level aerial mapping to micron level artifact scanning.

Gregory Dawe is known for his contributions to the CAVE Virtual Reality Theater and its derivatives, the ImmersaDesk, and PARIS. Dawe also did the mechanical design for and assembled the Varrier autostereographic display.

Ji Dai received his B.S. in 2013 from the Shanghai Jiao Tong University and his M.S. in 2015 from Boston University in the department of Electrical and Computer Engineering. He is currently a Ph.D. student at UC San Diego working on view interpolation and stereo panorama stiching methods with Professor Nguyen.

Truong Nguyen received his Ph.D. from Caltech in 1989 and came to the University of California San Diego in 2001. He manages the Video Processing Group and is a professor in the Signal Image Processing Program (SIP). He is a 1995 recipient of an NSF career award and is coauthor of a popular book: Wavelets and Filter Banks, and author of several matlab-based toolboxes on image compression, electrocardiagram compression, and filter bank design.

Harlyn Baker is a Consulting Scientist in the Robotics Laboratory of Stanfords Computer Science Department. He has a PhD in Computer Science from Urbana-Champaign, M.Phil. in Machine Intelligence from Edinburgh University, and BSc from Western Ontario in Canada. He has held academic positions at Edinburgh, Stanford, Heidelberg, and UI Illinois Chicago, and corporate roles at SRI International, Interval Research, Hewlett-Packard Laboratories, and EPIImaging, LLC.

Maxine Brown is the Director of the Electronic Visualization Laboratory (EVL) and the Software Technologies Research Center at University of Illinois at Chicago. Brown has been active in the ACM SIGGRAPH organization and in SIGGRAPH and ACM/IEEE Supercomputing conferences. In recognition of her services to UIC and the community at large, Brown is a recipient of the 1990 UIC Chancellors Academic Professional Excellence award; 2001 UIC Merit Award; and 1998 ACM SIGGRAPH Outstanding Service Award.

Thomas A. DeFanti, PhD, is a research scientist at the Qualcomm Institute, University of California, San Diego, and a distinguished professor emeritus of Computer Science at the University of Illinois at Chicago. He is recipient of the 1988 ACM Outstanding Contribution Award and was appointed an ACM Fellow in 1994. He shares recognition along with EVL director Daniel J. Sandin for conceiving the CAVE virtual reality theater in 1991.

Falko Kuester received a M.S.E. in Mechanical Engineering and Computer Science and Engineering from the University of Michigan, Ann Arbor, in 1994 and 1995 respectively and a Ph.D. in Computer Science from the UC Davis in 2001. He is a professor at UC San Diego, director of the UC San Diego DroneLab as well as the Cultural Heritage Engineering Initiative, advancing research in robotics, remote imaging, large-scale visual analytics and virtual reality.

JOIN US AT THE NEXT EI!

IS&T International Symposium on

Electronic Imaging

SCIENCE AND TECHNOLOGY

Imaging across applications . . . Where industry and academia meet!

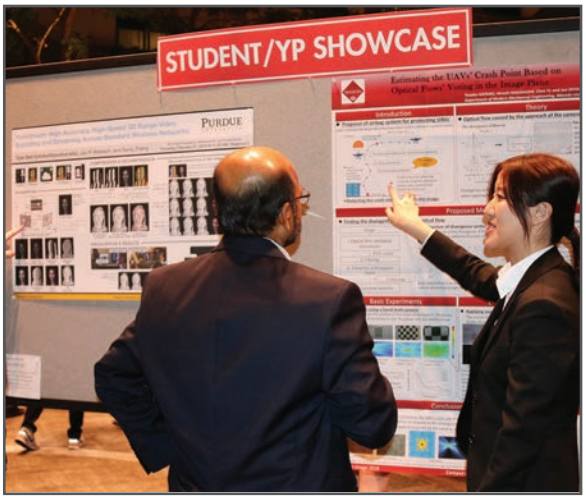

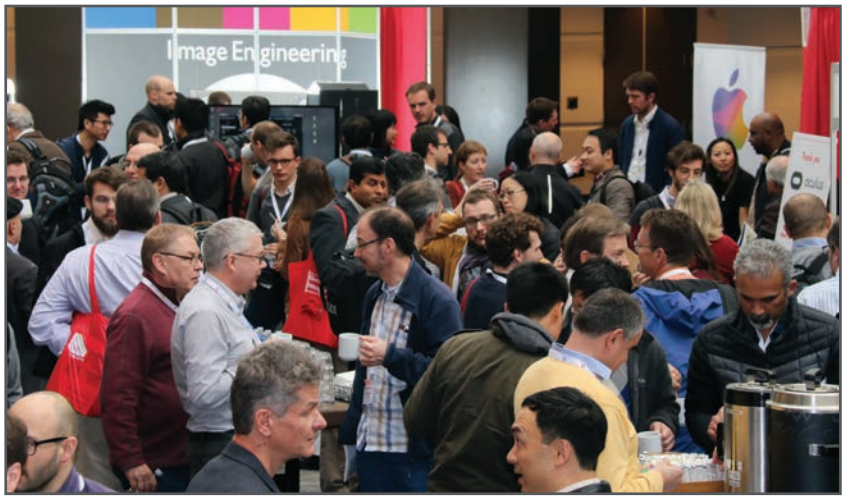

• SHORT COURSES • EXHIBITS • DEMONSTRATION SESSION • PLENARY TALKS •
• INTERACTIVE PAPER SESSION • SPECIAL EVENTS • TECHNICAL SESSIONS •

www.electronicimaging.org

IS&T
imaging.org